A R C H I V E S O F M E T A L L U R G Y A N D M A T E R I A L S
Volume 60 2015 Issue 3
DOI: 10.1515/amm-2015-0381

E. GUZIK*, D. KOPYCIŃSKI*#, W. WOŁCZYŃSKI**

GROWTH LAW FOR PERITECTIC PHASES FORMATION IN THE ZINC COATING

PRAWO WZROSTU FAZ PERYTEKTYCZNYCH W POWŁOCE CYNKOWEJ

Some experiments dealing with the isothermal hot dip galvanizing were carried out. The (Zn) – coating settled on the *Armco*-iron substrate were examined after arresting the solidification for different periods of time. The measurement of the thickness of each sub-layer in the coating were performed due to the SEM – analysis. The zinc segregation on the cross-section of the studied sub-layers were also determined by the EDS technique. The growth laws are formulated mathematically for each of the observed sub-layer. The mechanism of the sub-layer formation is also analysed due to the observation of the birth/nucleation of the phases in the sub-layers and the effect of flux onto the sub-layers morphology formation. The appearance of each phase is referred to the Fe-Zn diagram for stable equilibrium according to which these phases are the products of the adequate peritectic transformation.

Keywords: (Zn) – coating; zinc segregation; growth law; crystallization of peritectic phases

Przeprowadzono eksperymenty izotermicznego cynkowania zanurzeniowego. Powłoka (Zn) osadzona na żelazie *Armco* poddana została badaniom po zatrzymaniu krystalizacji dla różnych czasów trwania cynkowania. Dokonano pomiarów grubości każdej z podwarstw powłoki dzięki analizie SEM. Segregacja cynku na przekroju badanych podwarstw również została określona dzięki pomiarom przy użyciu techniki EDS. Sformułowane są matematycznie prawa wzrostu dla każdej z analizowanych podwarstw. Analizowany jest również mechanizm kształtowania podwarstw dzięki obserwacjom narodzin/zarodkowania poszczególnych faz w podwarstwach oraz dzięki analizie oddziaływania topnika na morfologię podwarstw. Formowanie każdej z faz jest odniesione do diagramu równowagowego Fe-Zn zgodnie z którym fazy te są produktami odpowiednich reakcji perytektycznych.

1. Introduction

A clarification of the mechanism responsible for the coatings formation enables the study on the hot-dip technology. The known analyses have proved that the coatings obtained from the hot-dip galvanizing are composed of two main layers, [1-13]. The first layer, directly contacting the substrate, is an alloyed layer usually composed of a few sub-layers of the intermetallic phases/compounds. The external layer, solidifying on the surface of the alloyed layer, is formed when the galvanized product is emerged from the bath, [10-15].

The Γ_1, δ and ζ – phase sub-layers grow on the steel substrate surface, within the first alloyed layer, as the product of peritectic transformations accompanying the (Zn) – coating solidification.

In the present study, this stage was examined in terms of the isothermal solidification until the critical time, after the lapse of which there is a transition from solidification to the first solid state transformation. The transformation may be described by a chemical reaction and examined as a consumption of the pro-peritectic phase by a predominant peritectic phase. For example the ζ – phase sub-layer is consumed by the δ – phase sub-layer. It leaves no doubt that in each case, an analysis of the zinc coating structure should be based on the Fe-Zn phase diagram for stable equilibrium and so far it has been the subject of numerous investigations [16,17].

* AGH UNIVERSITY OF SCIENCE AND TECHNOLOGY, FACULTY OF FOUNDRY ENGINEERING, 23 REYMONTA STR., 30-059 KRAKÓW, POLAND
** INSTITUTE OF METALLURGY AND MATERIALS SCIENCE, POLISH ACADEMY OF SCIENCES, 25 REYMONTA STR., 30-059 KRAKOW, POLAND
# Corresponding author:djk@agh.edu.pl

2. Methodology

The kinetics of zinc coating solidification was examined on properly selected samples, using a test stand designed especially for this purpose. The temperature was controlled and measured by a PID control unit with the Ni-CrNi thermocouple, ensuring stable zinc bath temperature with the ± 2°C accuracy.

Before dipping in the liquid zinc, the sample surface was chemically processed using products commonly applied in industry and the set of operations applied by galvanizing plants was examined in the following sequence: cleaning with degreasing – rinsing in water – etching in 15% aqueous solution of hydrochloric acid – rinsing in water – fluxing for 180 seconds (according to the technology applied in industry) in a solution composed of, among others, zinc chloride in an amount of up to 300 g/l and ammonium chloride in an amount of up to 150 g/l. The determined content of iron in flux was 0.41 g/l. The last operation before dipping in zinc bath was drying of the sample surface with flux coating applied onto it. The zinc bath was composed of electrolytic zinc containing (in mass percent as per the conformity certificate): 99.995%Zn, 0.0005%Pb, 0.0013%Cd, 0.0002%Fe, 0.0001%Sn, 0.0001%Cu, 0.0001%Al. The chemical composition of iron (in mass percent as per the conformity certificate) was: 0.036%C, below 0.01% Si, 0.01%P, 0.1%Mn, 0.09%Al, and Fe.

3. Mechanism of the (Zn) – coating formation

The sequence of the peritectic phase sublayers appearance was detected using the JEOL 500LV scanning electron microscope with attachment for the X-ray EDS microanalysis. The SEM microstructure of the zinc coating is shown in Fig. 1. This coating was obtained in the first few seconds after the immerging of the *Armco*-iron sample in the zinc bath. The qualitative and quantitative analysis has revealed that the dominant phase in the initial stage of coating solidification of the alloyed layer is the δ – phase sub-layer.

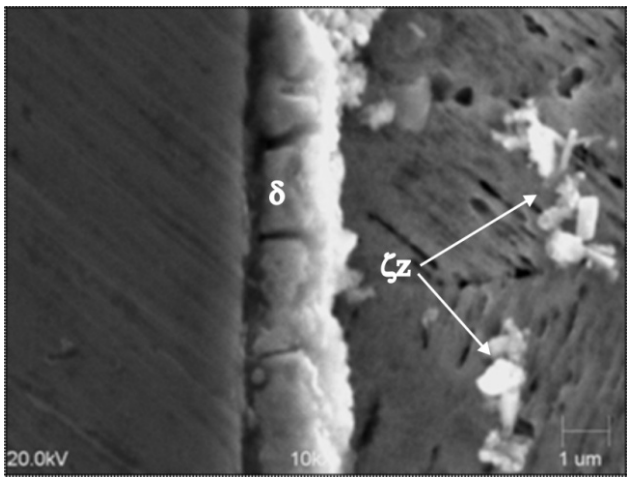

Fig. 1. Microstructure of the (Zn) – coating obtained on the *Armco*-iron substrate with the galvanizing time t = 11 seconds; SEM – analysis

It is assumed that the Γ_1 – phase sub-layer is formed almost at the same time as the δ – phase sub-layer, although sequentially, with the nucleation of the δ – phase, Fig. 2. Presumably, the Γ_1 – phase arises from the flux interaction and tends to fade within the observed time of process duration. As the time, t, elapses, the λ – thickness of the δ – phase sub-layer slightly increases. The coating obtained on samples immersed in the bath for a period of time from 9th second to 11th second, shows no traces of the presence of the crystals of the ζ – phase. Fig. 2 shows the microstructure of zinc coating formed in the 13th second. The formation of the first crystals of the ζ – phase on the surface of the already existing sublayer of the δ – phase is revealed, Fig. 2.

At the same time, together with the crystals of the ζ – phase forming on the surface of the sublayer the δ phase, some crystals of the ζ – phase also nucleate and grow in the bath, forming isolated precipitates characteristic for the so-called, hard zinc, ζ_Z, Fig. 1. Some precipitates of the hard zinc sink to the bottom of the tank to form removable sludge. At the same time, a part of the hard zinc joins the growing sublayer of the ζ – phase.

In further part of this study the ζ – phase solidification (hard zinc) is considered. This phase contacts the alloyed layer and is marked as the ζ_Z – sub-layer.

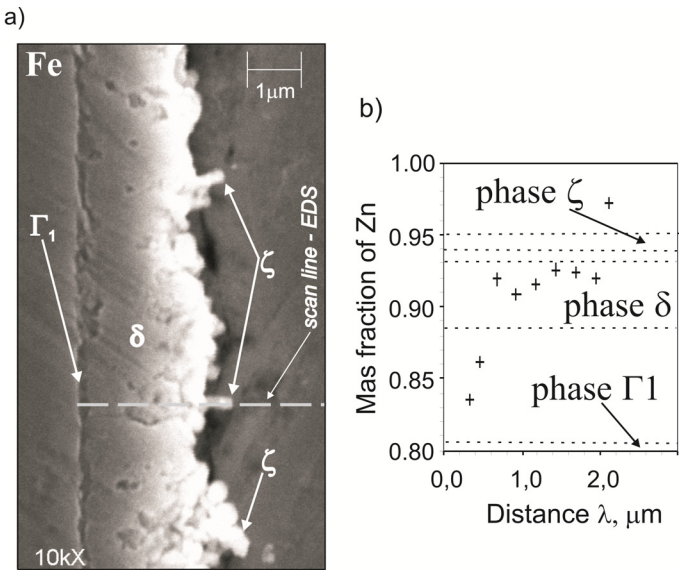

Fig. 2. Birth of the ζ – peritectic phase on the surface of the δ – peritectic phase in the 13-th second of the solidification process

Figure 3 shows the sequence of formation of the alloyed layer in the (Zn) – coating produced on the surface of the *Armco*-iron substrate at the time, t, of immersion in the bath from 30 seconds to 900 seconds. It should be noted that the values of time, t, adapted in the current study are comprised in a range designed by the technology of hot-dip galvanizing. A characteristic feature of SEM microstructure of the (Zn) – coating shown in Figure 3 is that the ζ – phase sub-layer dominates in the structure of the coating until the time, t_M. When the time t_M, is exceeded, due to a sudden change in the growth mechanism of a sublayer of the δ phase, its λ – thickness increases rapidly.

The δ – phase is again the dominant phase in the coating at time t = 300 s. At this time, the first solid / solid transformation begin to occur. Then, the sublayer of the δ – phase grow at the expense of the ζ – phase sub-layer, [1-13]. Qualitative analysis of the sequence of the coating formation allows estimating the time, t_M as equal to 300 seconds. A characteristic feature of the structure of the alloyed layer of the coating obtained at time, t > 300 seconds is the shape of the interface of the ζ – phase sub-layer, which from "random" transforms into a geometrical shape similar to the cellular one, Fig. 3. On the other hand, the Γ_1 – phase sublayer, having reached its maximum thickness, ceases to grow beyond the time, t_M.

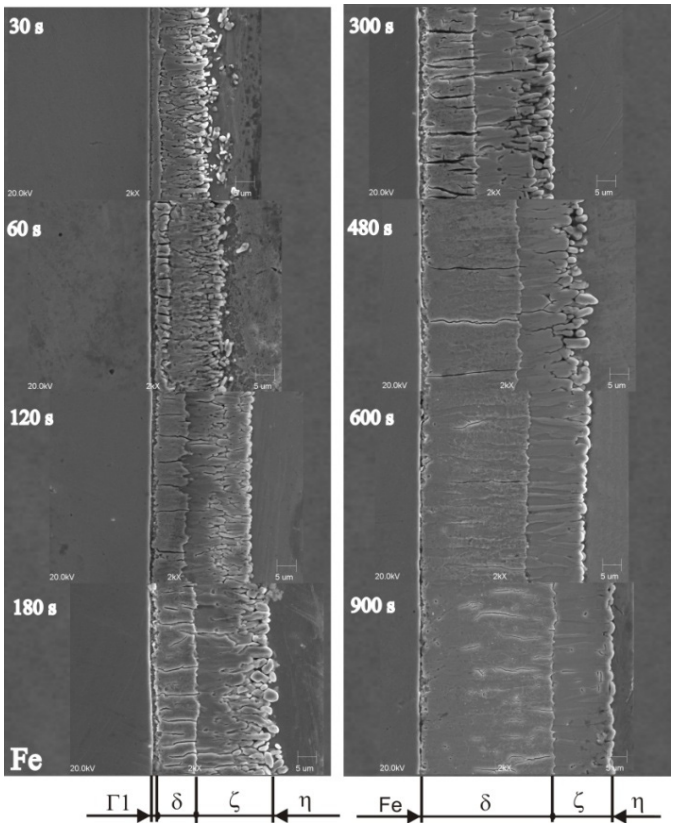

Fig. 3. Sequence of the alloyed layer formation on the surface of the *Armco*-iron observed within the period of time from 30th second to 900th second; SEM – analysis

4. Growth law for particular peritectic phases

The results of measurements of the λ-thickness for each peritectic phase sub-layer were used to develop the current model for the coating solidification. Also, the zinc concentration measured across each sub-layer of the coating was examined for different immersion times in the zinc bath, as shown in Fig. 4.

The measurement results for the time exceeding 300 seconds were disregarded due to the presence of structural perturbation resulting from the solid state transformations. Fig. 5 shows changes in the λ – total thickness of a double-layer of the ($\zeta + \zeta_Z$) – phases and also of the δ as well as Γ_1 – phase sublayers which were formed on the Armco-iron substrate. It should

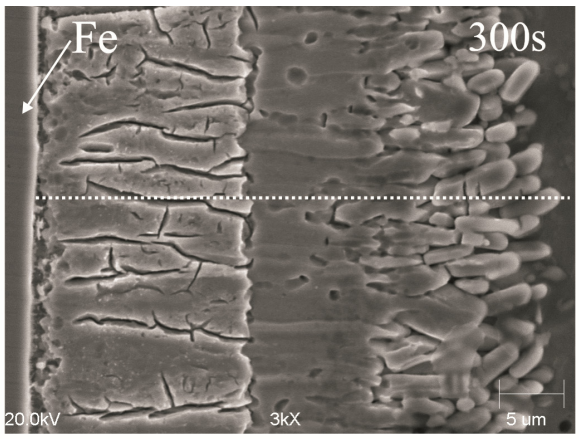

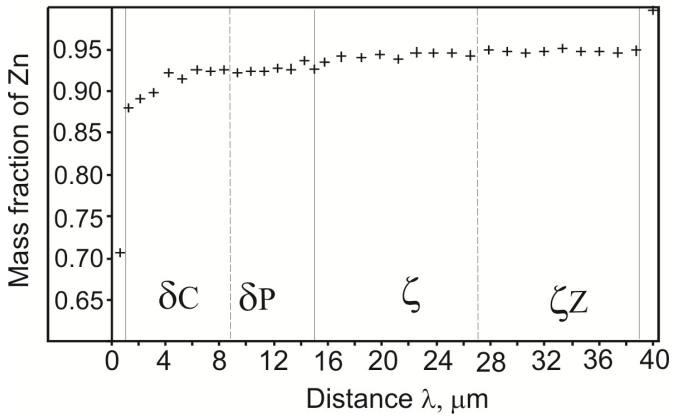

Fig. 4. Zinc segregation in the (Zn) – coating sub-layers with the approximate indication of the phase boundaries, as observed for time, t = 300 seconds

be emphasized that the ζ_Z phase had nucleated on the particles of ash present in the zinc bath. The ash was the product of the flux dissociation.

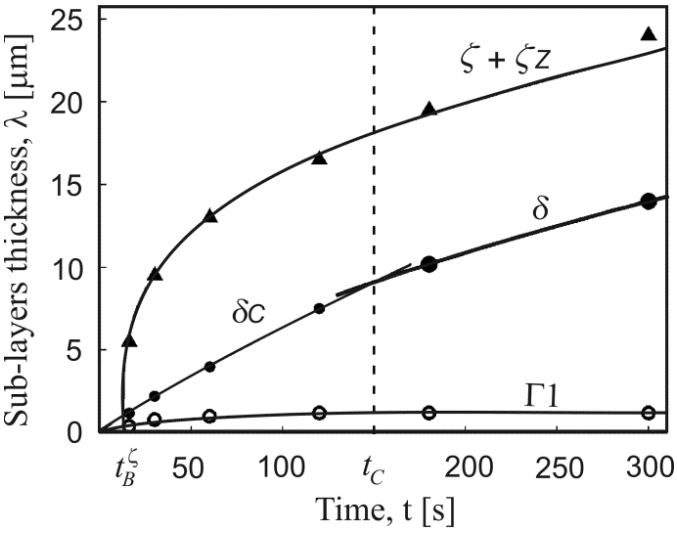

Fig. 5. Interpretation of measurement points for time t = 300 seconds, as selected for the solidification arrested by the "freezing" effect

When the thickness of coating is measured under industrial conditions, the technologist measures the ($\zeta + \zeta_Z$) – entire double

layer, without differentiating between the two growth mechanisms, i.e. the common one by exogenous solidification of the ζ – phase and the other one by endogenous solidification of the ζ_Z – phase. In this study, a distinction will be made between both mechanisms of the $(\zeta + \zeta_Z)$ – phase solidification, and the phase fraction simply called ζ – phase will be described by model. On the other hand, the fraction of the ζ – phase which is formed by the endogenous solidification will be neglected in the discussion of the coating thickening.

The behavior of the δ – phase sublayer thickening is divided into two ranges, Fig. 5. One can distinguish a set of points assigned to the kinetic curve, $\lambda(t)$, marking the range of the appearance of the phase designated as the δ_C – phase. The so-called compact morphology appears within the first range of the $\lambda(t)$ – curve (thin line denoted δ_C). Its appearance is accompanied by the so-called δ_P – palisade morphology formation. Therefore, the remaining part of the $\lambda(t)$ – curve (denoted δ) is dealing with the δ_P – palisade morphology formation, only. Both morphologies of the δ – phase are designated by one common symbol, δ, corresponding to the Fe-Zn phase diagram for stable equilibrium, [16,17].

The δ phase as a total of both compact and palisade morphologies are indicated by the thick line, Fig. 5. Both kinetics curves intersect each other at a point defined by the t_C – time which is the critical time for the hot dip galvanizing technology.

The t_C – critical time indicates that at this moment (of approximately 150th second) the particles of flux and of its ash have ceased to exist after being burnt out in the bath and there is no substrate for nucleation which would generate the ζ_Z – phase formation by the endogenous solidification. Since that time, the sub-layer of the ζ_Z – phase continues its existence but without increasing its thickness. In structure images it is visible as a sublayer of loose structure with wide channels between the grains, Fig. 4. It follows that also the sub-layer of the Γ_1 – phase is growing until certain moment, Fig. 5. An interpretation of the sequence of its formation indicates that it grows until the certain time to exist later only as a sub-layer of constant thickness, Fig. 3. Therefore, a second hypothesis is proposed according to which the Γ_1 – phase formation is somehow related with the use of flux in this technology.

It can be shown that Γ_1 – phase nucleates on the substrate of the *Armco*-iron, whereas the δ – phase nucleates on the surface of the Γ_1 – phase almost at the same time, although sequentially. First, it was demonstrated by applying SEM, Fig. 1, Fig. 2, and next, concluded in the studies of the growth model that the ζ – phase arises a little later, i.e. at the time indicated t_B^{ζ}, Fig. 5. The t_B^{ζ} – time determines the birth of the ζ – phase. It occurs at about –13th second, Fig. 2, under assumption that the formation of the Γ_1 – phases takes place at the time, $t_B^{\Gamma_1} = 0$.

One can also conclude that the formation of the δ_C – phase formation is driven by two reasons: by the impact of flux and its ash on solidification and by the growth of the Γ_1 – phase. After the lapse of the t_C – critical time, the solidification returns to its normal state and the δ_P – palisade phase arises. A common image of both the δ_C and δ_P morphologies, or in other words, of their sum is – as already mentioned – the δ – phase, and so the phase such as the one described by the phase diagram for stable equilibrium.

So, from the choice of functions for experimental points it follows that:

- for the Γ_1 – phase the growth law assumes an elliptical form, with exponential function constituting its main element:

$$\lambda^{\Gamma 1}(t) = G\left(2(t_C - t_B^{\Gamma 1})(t - t_B^{\Gamma 1}) - (t - t_B^{\Gamma 1})^2\right)^g \tag{1}$$

  where: $t_B^{\Gamma_1} \le t \le t_C$ and $G = 0.005$, $g = 0.55$
- for the ζ_Z – phase the growth law has also an elliptical form (though it is a very rough approximation); the analysis presented here states only the law of the growth of the ζ_Z – phase because, as already mentioned, this phase is formed by the endogenous solidification on nuclei:

$$\lambda^{\zeta Z}(t) = R\left(2(t_C - t_B^{\zeta})(t - t_B^{\zeta}) - (t - t_B^{\zeta})^2\right)^r \tag{2}$$

  where: $t_B^{\zeta} \le t \le t_C$ and $R = 1.383$, $r = 0.20$;
- for the δ_C – phase the growth law is fully exponential:

$$\lambda^{\delta C}(t) = C\left(t - t_B^{\delta}\right)^c \tag{3}$$

  where: $t_B^{\delta} \le t \le t_C$ and $C = 0.106$, $c = 89$;
- for the δ – phase the growth law is also fully exponential:

$$\lambda^{\delta}(t) = D\left(t - t_B^{\delta}\right)^d \tag{4}$$

  where: $t_B^{\delta} \le t$ and $D = 0.408$, $d = 0.62$;
- for the ζ – phase the growth law is also fully exponential:

$$\lambda^{\zeta}(t) = Z\left(t - t_B^{\zeta}\right)^z \tag{5}$$

  where: $t_B^{\zeta} \le t$ and $Z = 0.390$, $z = 0.62$;

The following values of the parameters have been applied in calculations: $t_B^{\Gamma_1} = 0$, $t_B^{\delta} = 3$, $t_B^{\zeta} = 13$, $t_C = 150$.

It is worth noting that during the period when only the δ_P – palisade phase and ζ – phase coexist, that is, after the lapse of the t_C – critical time, the exponents in both growth laws are identical to each other and equal to 0.62. Moreover, the value of the D/Z ratio is exactly equal to the value of the ratio of both thicknesses of the considered phases. The g – exponent is close to 0.5, which means that the Γ_1 – phase is formed by the bulk diffusion through the mass of the Γ_1 – phase sublayer. The c – parameter for the δ_C – phase has already acquired a value closer to 1, which means that it grows occurs mainly by diffusion along the cells boundaries (grooves).

Therefore, the Γ_1 – phase should have cells with internal channels for the bulk diffusion, Fig. 6, whereas the morphology of the δ_C – phase should have small cells without internal channels but with large grooves, Fig. 7.

The difference between the δ_C – phase and δ_P – phase morphologies is shown in Fig. 8c. The difference in the morphologies of the delta δ_C and δ_P – phases is confirmed by the EDS analysis of zinc segregation, Fig. 8a.

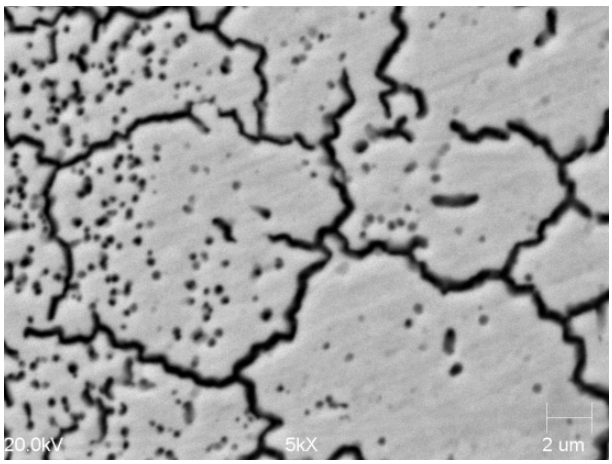

Fig. 6. Cross-section of the Γ_1 – phase sub-layer showing internal the channels within the cells; SEM – analysis

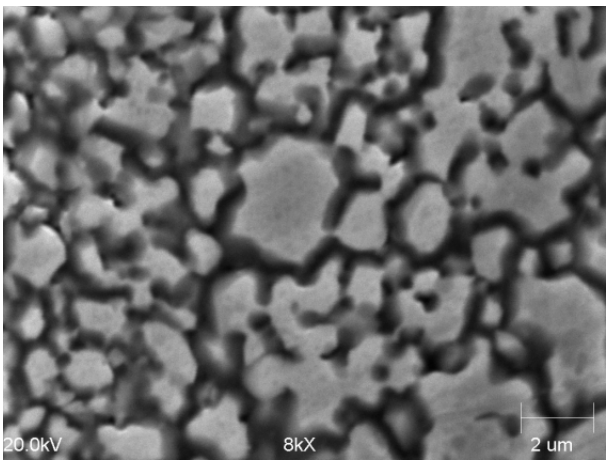

Fig. 7. Cross-section of the δ_C – phase sub-layer showing cells surrounded by the large grooves; SEM analysis

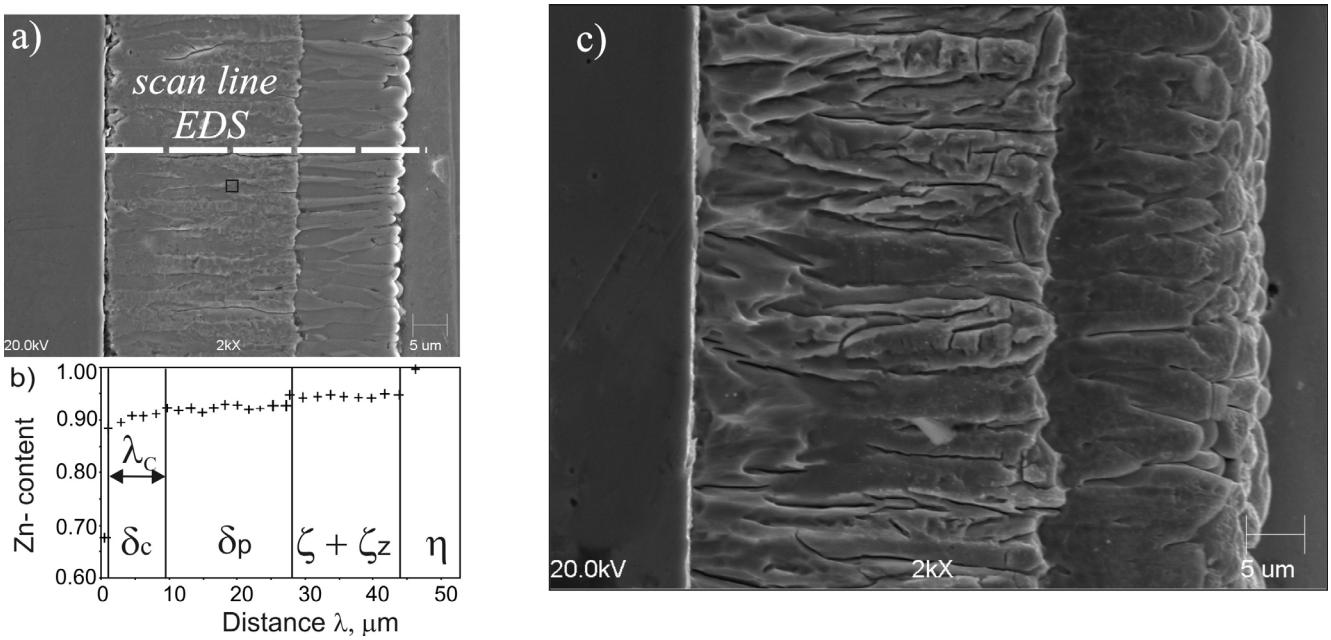

Fig. 8. (Zn) – coating, a) the Zn – segregation across the coating sub-layers; EDS analysis after initial etching, c) coating morphology after deep etching; SEM analysis

5. Concluding remarks

1. Even the isothermal formation of peritectic phases in the (Zn) – coating with the presence of significant undercooling, fully reflects the analogous sequence of solidification and phases appearance consistent with the Fe-Zn phase diagram for stable equilibrium.
2. The kinetics of the formation of peritectic phases in the (Zn) – coating was described by means of the adequate growth laws according to which some sub-layers are formed mainly by the bulk diffusion whereas the others by a significant contribution of the boundary diffusion.
3. The current growth laws are in good agreement with the analogous laws presented recently for the same technology, [18].
4. The EDS – measurement of the zinc segregation on the cross-section of the coating together with SEM – analysis allowed to identify precisely the morphological differences among the studied phase sub-layers and to conclude when the effect of flux and its ash on the coating morphology is completed.

Acknowledgements

The financial support was provided by the National Center for Research and Development under Grant No. **DEC-2012/05/B/ST8/00100.**

REFERENCES

[1] W. Wołczyński, E. Guzik, D. Kopyciński, C. Senderowski, Mechanism of the Intermetallic Phase/Compound Growth on the Substrate, Journal of Achievements in Materials and Manufacturing Engineering **24**, 324-327 (2007).

[2] A.R. Marder, The Metallurgy of Zinc-Coated Steel, Progress in Materials Science **45**, 191-271 (2000).

[3] R. Parisot, S. Forest, A. Pineau, F. Grillon, X. Démonet, J.M. Mataigne, Deformation and Damage Mechanisms of Zinc Coatings on Hot-Dip Galvanized Steel Sheets, Metallurgical and Materials Transaction **35A**, 797-811 (2004).

[4] J. Inagaki, M. Sakurai, T. Watanabe, Alloying Reactions in Hot-Dip Galvanizing and Galvannealing Processes, ISIJ International **35**, 1388–1393 (1995).

[5] C.R. Xavier, U.R. Seixas, P.R. Rios, Further Experimental Evidence to Support a Simple Model for Iron Enrichment in Hot-Dip Galvanneal Coatings on IF Steel Sheets, ISIJ International **36**, 1316-1327 (1996).

[6] J.D. Culcasi, P.R. Sere, C.I. Elsner, A.R. Sarli, Control of the Growth of Zinc – Iron Phases in the Hot-Dip Galvanizing Process, Surface and Coatings Technology **122**, 21-23 (1999).

[7] W. Wołczyński, E. Guzik, J. Janczak-Rusch, D. Kopyciński, J. Golczewski, H.M. Lee, J. Kloch, Morphological Characteristics of Multi-Layer/Substrate Systems, Materials Characterization **56**, 274-280 (2006).

[8] W. Wołczyński, T. Okane, C. Senderowski, D. Zasada, B. Kania, J. Janczak-Rusch, Thermodynamic Justification for the Ni/Al/Ni Joint Formation by a Diffusion Brazing, International Journal of Thermodynamics **14**, 97-105 (2011).

[9] W. Wołczyński, T. Himemiya, D. Kopyciński, E. Guzik, Solidification and Solid/Liquid Interface Paths for the Formation of Protective Coatings, Archives of Foundry Engineering **6**, 359-362 (2006).

[10] D. Kopyciński, E. Guzik, W. Wołczyński, Coating (Zn) Formation during Hot-Dip Galvanizing, Inżynieria Materiałowa **164**, 289-292 (2008).

[11] D. Kopyciński, TMS 2013 Annual Meeting, Crystallization of Intermetallic Phases Fe-Zn during Hot-Dip Galvanizing Process, TMS2013 Supplemental Proceedings, 439-446.

[12] D. Kopyciński, E. Guzik, Intermetallic Phases Formation in Hot Dip Galvanizing Process, Solid State Phenomena **197**, 77-82 (2013).

[13] D. Kopyciński, A. Szczęsny, The Effect of Ductile Cast Iron Matrix on Zinc Coating during Hot Dip Galvanizing of Castings, Archives of Foundry Engineering **12**, 101-104 (2012).

[14] A. Quiroga, S. Claessens, B. Gay, M. Rappaz, A Novel Experiment for the Study of Substrate-Induced Nucleation in Metallic Alloys, Metallurgical and Materials Transactions **35A**, 3543-3550 (2004).

[15] J. Strutzenberger, J. Faderl, Solidification and Spangle Formation of Hot-Dip Galvanizing Zinc Coatings, Metallurgical and Materials Transactions **29**, 631-646 (1998).

[16] K. Mita, T. Ikeda, M. Maeda, Phase Diagram Study of Fe-Zn Intermetallics, Journal of Phase Equilibria **23**, 1808-1815 (2000).

[17] X. Su, N.Y. Tang, J.M. Toguri, A Study of the Zn-Rich Corner of the Zn-Fe-Sn System, Journal of Phase Equilibria **26**, 528-532 (2003).

[18] W. Wołczyński, B. Kucharska, G. Garzeł, A. Sypień, Z. Pogoda, T. Okane, Part III. Kinetics of the (Zn) – Coating Deposition during Stable and Meta-Stable Solidifications, Archives of Metallurgy and Materials **60**, 199-207 (2015).

Received:20 April 2015.